International Journal of Refrigeration 151 (2023) 136–145

Contents lists available at ScienceDirect

International Journal of Refrigeration

journal homepage: www.elsevier.com/locate/ijrefrig

pvTx properties for carbon dioxide (CO_2)/difluoromethane (R32)/ 1,1,1,2-tetrafluoroethane (R134a) ternary mixture measured in the compressed liquid, superheated vapour, and two-phase regions

Propriétés PVTx du mélange ternaire dioxyde de carbone (CO2)/difluorométhane(R-32)/ 1,1,1,2-tétrafluoroéthane (R-134a) mesuré à l'état de liquide comprimé, de vapeur surchauffée et diphasique

L. Fedele [a], G. Di Nicola [a,b], D. Menegazzo [a,c], S. Tomassetti [b,*], S. Bobbo [a], P. Quattrocchi [d], L. Alemanno [d], L. Catanzani [d], S. Amato [d]

[a] *Construction Technologies Institute, National Research Council,(ITC-CNR), Padova, Italy*
[b] *Department of Industrial Engineering and Mathematical Sciences, Marche Polytechnic University, (UnivPM), Ancona, Italy*
[c] *Department of Industrial Engineering, University of Padua,(UNIPD), Padova, Italy*
[d] *Angelantoni Test Technologies S.r.l, Massa Martana, (PG), Italy*

ARTICLE INFO

Keywords:
Equations of state
Ultra-low temperature
Carbon dioxide (R744)
Ternary system
R472A
Mots clés:
Équations d'état
Température très basse
Dioxyde de carbone (R-744)
Système ternaire
R-472A

ABSTRACT

In low-temperature refrigeration applications, mixtures containing carbon dioxide and refrigerants with low triple points are considered potential substitutes for the refrigerant R23, characterised by a very high global warming potential. This study provides *pvTx* measurements for the ternary mixture of carbon dioxide (CO_2), difluoromethane (R32), and 1,1,1,2-tetrafluoroethane (R134a) carried out in the compressed liquid, superheated vapour, and two-phase regions. A vibrating tube densimeter was used to measure the compressed liquid density along eight isotherms evenly spaced from (283.15 to 353.15) K and for pressures from near saturation up to 35 MPa. An isochoric apparatus was used to measure the two-phase and superheated vapour *pvTx* properties along three isochores from (223.15 to 303.15) K. The measurement uncertainties were estimated to be lower than 1 $kg \bullet m^{-3}$ for the liquid density and 0.02 $m^3 \bullet kg^{-1}$ for the vapour specific volume. All the presented properties were compared with the calculations of the multi-fluid Helmholtz-energy explicit model. Both the default binary interaction parameters available in REFPROP 10.0 and new binary interaction parameters tuned on the presented data and the experimentally-determined thermodynamic properties collected from the literature have been used in the model. The tuned parameters provided lower deviations than the default parameters used in REFPROP 10.0.

1. Introduction

The COVID-19 pandemic raised the need for reliable systems for the transport and storage of vaccines. Each proposed vaccine has different requirements for storage, preparation, and management. The two leading vaccines (Pfizer Biontech and Moderna) are required to be frozen till −80 °C during transportation (Santos et al., 2021; Sun et al., 2021). This context renewed the attention to ultra-low temperature (ULT) equipment, used for food products, biological samples, and medicines. Although working fluids for ULT systems are not subject to Regulation (EU) No. 517/2014 (2014), many ULT working fluids are HFCs and would be counted toward the HFC phase-down specified by the Kigali Amendment (UNEP, 2016) stating to globally reduce the production and the consumption of HFCs since 2018. This led to an increase in HFCs price in Europe for the most widespread refrigerants.

To reach ultra-low temperature, while rejecting heat at ambient temperature level, two-stage cascade systems are commonly used;

* Corresponding author.
E-mail address: s.tomassetti@univpm.it (S. Tomassetti).

https://doi.org/10.1016/j.ijrefrig.2023.04.001
Received 10 November 2022; Received in revised form 31 March 2023; Accepted 2 April 2023
Available online 7 April 2023

Nomenclature

Symbols

T	Temperature
p	Pressure
ρ	Density
R	Molar gas constant
v	Specific volume
w	Mass fraction
x	Liquid mole fraction
y	Vapour mole fraction
c_p	Isobaric specific heat
δ	Reduced density
Δ	Deviation
τ	Reduced temperature
β, γ	Binary interaction parameters
α	Dimensionless Helmholtz free energy

Subscripts

c	Critical
T	Temperature
v	Specific volume
r	Residual
exp	Experimental
calc	Calculated

single-stage equipment is less widespread but can be used too. In two-stage cascade systems, two different refrigerants work in two different circuits, coupled by a heat exchanger which works as an evaporator for the top cycle (i.e., the cycle working at high evaporating temperature) and as a condenser for the bottoming cycle (i.e., the cycle working at low evaporating temperature). For these applications R23 and R508B (R116/R23, 54/46 mass%) are commonly used for the bottoming cycle (Mota-Babiloni et al., 2020); however, they are characterised by very high GWPs: the value of R23 is 14,800 and the value of R508B is 13,400. CO_2 is an interesting alternative for the bottoming cycle, if the system requires an evaporating temperature greater than 218 K, otherwise frost issues could occur on the refrigerant itself. Mixing CO_2 with refrigerants characterised by a lower triple point offers an interesting solution to the substitution issues (Di Nicola et al., 2011, 2005a).

The experimentally determined thermophysical properties of refrigerants mixtures are crucial to develop reliable equations of state and models for their transport properties. Accurate models are necessary to design refrigeration systems and to analyse their thermal performances. Various thermophysical property measurements for several binary systems containing CO_2 and conventional or natural refrigerants are available in the literature (Arami-Niya et al., 2020). In contrast, a very limited number of measurements for the multicomponent systems containing CO_2 were found in the literature. Arami-Niya et al. (2020) measured the vapour-liquid equilibrium (VLE), the liquid-phase density, and the liquid-phase heat capacity for the CO_2/R1234yf/R32 ternary system and the CO_2/R1234yf/R32/R125/R134a 5-component system. Viscosity and thermal conductivity measurements for the same multicomponent systems were reported by Yang et al. (2020) and Kim et al. (2020), respectively.

Table 2
Target and measured mass fractions (w) of CO_2/R32/R134a ternary system.

	w_{CO2}	w_{R32}	w_{R134a}
Target composition	0.69	0.12	0.19
Composition of bottle 1	0.694	0.120	0.186
Composition of bottle 2	0.684	0.117	0.199

In this work, the thermodynamic properties of the ternary system consisting of 69 mass% of CO_2, 12 mass% of R32, and 19 mass% of R134a are measured. The studied mixture, classified as R472A in the ASHRAE Standard 34 (ASHRAE, 2019), has a GWP of 350 and is non-flammable and of low toxicity. Therefore, it is proposed as a potential low GWP alternative for R23 in ULT applications, such as environmental chambers, freeze dryers, and very low temperature storages. Specifically, due to its favourable thermodynamic properties down to 213.15 K, R472A is particularly suitable for automotive environmental testing (i.e., battery test chambers).

A vibrating tube densimeter was used to measure the mixture's compressed liquid density along 8 isotherms evenly spaced from (283.15 to 353.15) K and for pressures from near saturation up to 35 MPa. The two-phase and superheated vapour *pvTx* properties were measured through an isochoric apparatus along 3 isochores from (223.15 to 303.15) K. Then, a comparison between the presented measurements and the calculations of the multi-fluid Helmholtz-energy explicit model is reported. The binary interaction parameters available in REFPROP 10 and the binary interaction parameters tuned in this work are tested and used. The tuning of the parameters is performed through a heuristic optimisation algorithm, including the presented measurements and the data of the binary mixtures constituting the ternary mixture available in the literature. Finally, the results of preliminary experimental testing of R472A using an environmental simulation chamber are shown.

2. Experimental section

2.2. Materials

Table 1 reports details regarding the samples of CO_2 (carbon dioxide, CO_2, CAS number 124–38–9), R32 (difluoromethane, CH_2F_2, CAS number 75–10–5), and R134a (1,1,1,2-tetrafluoroethane, $C_2H_2F_4$, CAS number 811–97–2) measured in this work. The samples were analysed with a gas chromatograph having a thermal conductivity detector, and the results are shown in Table 1. To eliminate the non-condensable gases, the samples of the pure refrigerants were subjected to cycles of freezing, evacuation, thawing, and ultrasonic stirring.

The ternary mixture was gravimetrically prepared by the following procedure. To determine the charged mass of each refrigerant, the initial bottle was weighted with a balance (uncertainty of $\pm$ 0.1 g) in each step of the charging procedure. Firstly, R134a was charged, then R32, and finally CO_2. To ensure that the composition of the liquid in the bottle was approximately equal to the bulk composition of the prepared mixture, the bottle volume was almost entirely filled with the ternary mixture in the liquid phase, avoiding overpressurizing the bottle. Before charging the apparatus, the sample bottle underwent mechanical stirring for few hours. Two different sample bottles were used for the density and *pvTx* measurements. The mass fractions, *w*, of the mixture samples loaded into the bottle used to charge the vibrating tube

Table 1
Descriptions of CO_2, R32 and R134a samples.

Chemical Name	ASHRAE Designation	CAS Number	Source	Initial Mole Fraction Purity	Final Mole Fraction Purity
Carbon dioxide	R744	124–38–9	Sol SpA	0.9999	0.9999
Difluoromethane	R32	75–10–5	Ausimont Spa	0.9999	0.9999
1,1,1,2-Tetrafluoroethane	R134a	811–97–2	Ausimont Spa	0.9998	0.9999

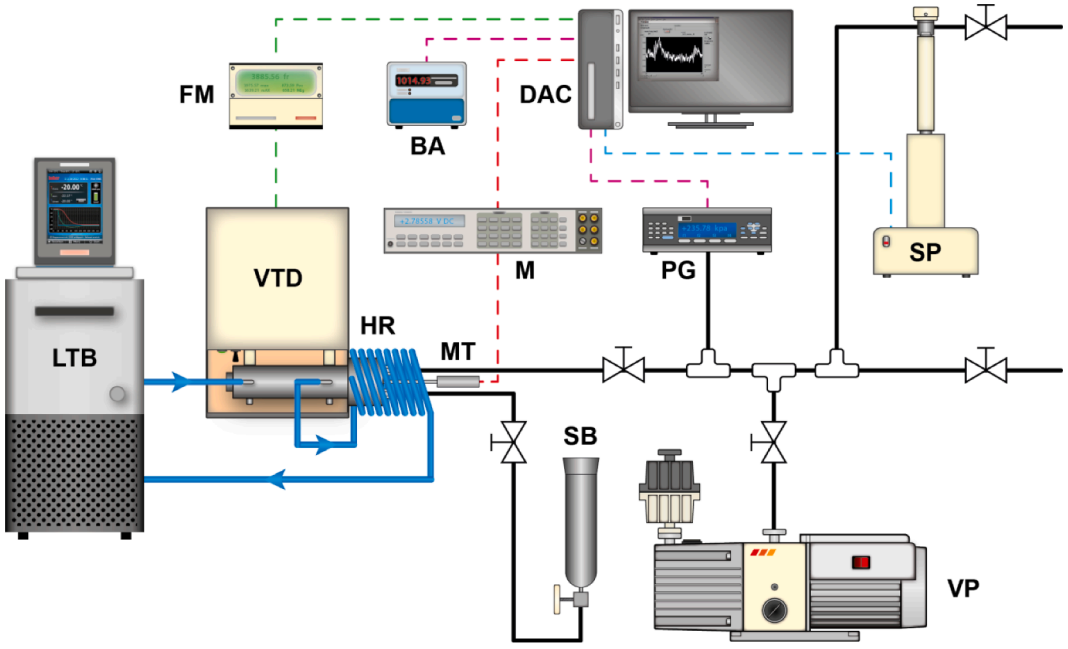

LTB	Liquid thermostatic bath	BA	Atmospheric barometer
FM	Frequency meter	DAC	Data acquisition and control
VTD	Vibrating tube densimeter	M	Multimeter
HR	Heat Exchanger	PG	Pressure gauge
MT	Thermometer	SP	Syringe pump
SB	Sample bottle	VP	Vacuum pump

Fig. 1. Compressed liquid density apparatus scheme.

Table 3
Experimental uncertainties for the measurements performed with the compressed liquid density apparatus.

Pressure uncertainty	10 kPa
Temperature stability	±0.003 K
Temperature uncertainty	0.05 K
Density uncertainty	0.4–0.6%

densimeter (bottle 1) and the isochoric apparatus (bottle 2) are shown in Table 2. From the propagation of the uncertainty, the uncertainties for the mass fractions were estimated to be around 0.005.

2.3. Compressed liquid density apparatus

The compressed liquid density measurements were carried out at CNR-ITC by means of a stainless-steel vibrating tube densimeter (Anton Paar DMA 512). Since the apparatus (shown in Fig. 1), procedure, and calibration have been described in detail elsewhere (Bobbo et al., 2004, 2002; Fedele et al., 2018), we will provide only a very short description below.

Firstly, the system was purged with nitrogen and evacuated. Then, the sample bottle was completely discharged into the vibrating tube and the measurement circuit, charging from the liquid phase to avoid any phase change composition. The target temperature was set by means of a thermostatic bath and the mixture was compressed to 35 MPa by the syringe pump. Once temperature and pressure were both stable, the period of vibration together with temperature and pressure were acquired by means of a dedicated LabView acquisition system. Then, the syringe pump brought the blend to the next target pressure and the procedure was repeated. A calibration equation was used to correlate the oscillation period of the vibrating tube with the sample density. The calibration equation is a function of temperature and pressure, and it was determined by measuring the oscillation period of the densimeter U-tube under vacuum and with water. The choice of water as a calibration fluid was due to the availability of high-accuracy EoS by Wagner and Pruß (2002). A piezoresistive transducer Druck DPI 145 was used to measure the sample pressure, while a Pt100Ω resistance thermometer measured the temperature. Table 3 shows an overview of experimental uncertainties and the combined standard uncertainty on compressed liquid density.

2.4. pvTx apparatus

The two-phase and superheated vapour *pvTx* measurements have been carried out at Università Politecnica delle Marche (UnivPM) by using an isochoric apparatus. Since the experimental setup, the measurement procedure, and the measurement uncertainties have been described in detail elsewhere (Brown et al., 2017; Di Nicola et al., 2005b; Giuliani et al., 1995), we present only a summary description here.

As shown in Fig. 2, the main components of the isochoric apparatus are the following:

- One isochoric sphere made of AISI 304 stainless steel connected to a magnetic pump for mixing the charged sample.
- One differential Ruska 7000 pressure transducer coupled with an electronic null indicator and connected to the sphere. The total volume of the measuring cell (including the tubing, the pressure transducer cavity, and magnetic pump) is about 273.5 cm^3 at 298 K.
- Two thermostatic baths to perform measurements from (210 to 380) K.

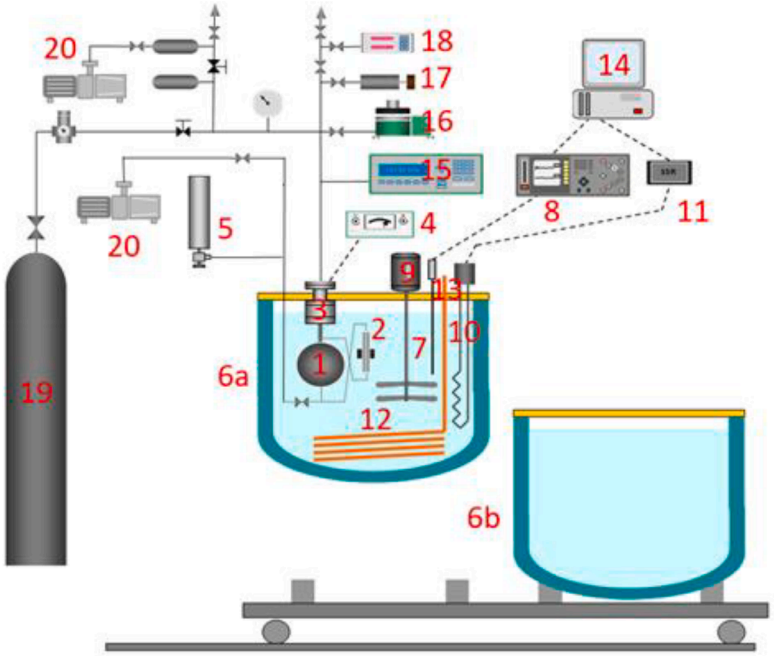

1	Constant volume spherical cell	11	Power system
2	Magnetic pump	12	Cooling coil
3	Differential pressure transducer	13	Connections to auxiliary thermostatic bath
4	Electronic null indicator	14	Acquisition system
5	Charging system	15	Bourdon gage
6	Thermostatic baths	16	Dead weight gage
7	Platinum thermo-resistances	17	Vibrating cylinder pressure gage
8	Thermometric bridge	18	Precision pressure controller
9	Stirrer	19	Nitrogen reservoir
10	Heater	20	Vacuum pump system

Fig. 2. Isochoric apparatus scheme.

Table 4
Experimental uncertainties for the measurements performed with the isochoric apparatus.

Pressure uncertainty	0.5 kPa
Temperature uncertainty	0.015 K
Volume uncertainty	0.15 cm^3
Mass uncertainty	0.05 g
Specific volume uncertainty	0.0008–0.0165 $m^3 \bullet kg^{-1}$

- One PID controller with a 25 Ohm platinum resistance thermometer (Hart Scientific 5680) used to maintain the set-point temperature.

The experimental uncertainties for the temperature, pressure and volume measurements are reported in Table 4.

The gravimetric method was used to fill the isochoric sphere with the measured samples. As a first step, the bottle containing the mixture sample, prepared as explained above, and an evacuated bottle were weighed with a Sartorius MC 1 electronic balance (uncertainty of 0.025 g). Then, they were connected to the apparatus. The charging bottle was connected in an inverted position to be sure to charge the liquid phase of the mixture into the measuring cell. After evacuating the isochoric sphere, connections, and tubing, a set sample amount was charged into the measuring cell. For all the measured isochores, a limited amount of liquid sample was discharged from the charging bottle to ensure that the bottle volume filled with the ternary mixture in the vapour phase was very small. In this way, the composition of the sample charged in the apparatus was very close to the bulk composition of the mixture in the sample bottle. Then, the mass standing in the tubing and connections was recovered by means of the evacuated bottle. After disconnecting the two bottles from the system, they were weighed again. The difference between the bottles' initial and final masses allowed us to determine the sample amounts discharged from the charging bottle and recovered with the evacuated bottle. Consequently, the mass loaded into the isochoric sphere was determined by subtracting the recovered mass from the discharged mass. Table 4 shows the uncertainty for the mass measurements. As explained in previous works (Brown et al., 2018, 2017), the combined standard uncertainties for the specific volume measurements were estimated through the propagation of uncertainty and are reported in Table 4.

The measurements at a specific temperature set-point were performed by the following procedure. After the thermostatic bath's temperature was stable, a circulating pump was turned on for few minutes. Then, the charged mass was allowed to stabilise for over an hour and the pressures were recorded. Next, the measurements at another temperature set-point were carried out by changing the thermostatic bath temperature and repeating the procedure.

Table 5
Measured temperature (T) pressure (p) and compressed liquid density (ρ) for the ternary mixture.[a].

T/K	p/kPa	ρ/ kg m $^{-3}$	T/K	p/kPa	ρ/ kg m $^{-3}$
283.15	6009	984.3	323.15	10,012	734.1
283.15	7499	994.9	323.15	15,008	840.8
283.15	10,001	1011.0	323.15	20,017	893.8
283.15	15,007	1036.9	323.15	23,199	920.8
283.15	20,009	1058.1	323.15	25,019	930.8
283.15	25,008	1076.3	323.15	30,004	959.6
283.15	30,012	1092.3	323.15	35,010	983.5
283.15	35,001	1106.7			
293.15	7510	939.1	333.15	10,022	566.6
293.15	10,012	961.6	333.15	15,021	773.7
293.15	15,013	994.8	333.15	17,506	813.6
293.15	20,015	1020.5	333.15	20,004	843.6
293.15	25,010	1041.9	333.15	25,012	888.6
293.15	30,005	1060.2	333.15	30,017	922.4
293.15	34,989	1076.5	333.15	35,010	949.6
303.15	7510	869.0	343.15	10,003	393.7
303.15	10,018	904.7	343.15	15,000	690.6
303.15	15,017	949.9	343.15	20,011	787.0
303.15	15,001	950.0	343.15	25,014	843.5
303.15	20,017	982.2	343.15	29,998	884.8
303.15	25,014	1007.8	343.15	34,998	916.0
303.15	30,003	1029.2			
303.15	35,003	1047.8			
313.15	7504	763.2	353.15	9989	315.9
313.15	10,005	832.3	353.15	15,089	612.0
313.15	15,007	897.9	353.15	20,001	729.7
313.15	19,999	938.8	353.15	25,010	798.6
313.15	25,015	969.7	353.15	29,988	845.3
313.15	30,013	994.7	353.15	35,010	881.3
313.15	34,985	1015.9			

[a] Standard uncertainties are $u(T)$=0.05 K, $u(p)$=10 kPa and $u(\rho)$=0.4–0.6%.

3. Results

3.1. Compressed liquid density

The compressed liquid density of the ternary mixture CO_2/R32/R134a was measured from 283.15 K up to 353.15 K with 10 K steps and from pressures near saturation up to 35 MPa. The experimental results are summarised in Table 5 and shown in Fig. 3.

3.2. PvTx measurements

The two-phase and superheated vapour *pvTx* properties of CO_2/R32/R134a ternary system were measured along 3 isochores (0.0643, 0.1556, 0.3002) m^3 kg^{-1}, in the temperature range from (223.15 to 303.15) K. The *pvTx* measurements in the two-phase and superheated vapour regions are shown in Fig. 4. Their *T, p* behaviours allow discerning the two-phase measurements from those in the superheated vapour region. The two-phase and the vapour-phase measurements are reported in Tables 6 and 7, respectively.

4. Data elaboration and correlation

4.1. Comparison with REFPROP 10.0

Experimental data were compared with calculated data of REFPROP 10.0 and the deviations are shown in Figs. 5 and 6 for compressed liquid density and for two-phase and superheated vapour density, respectively. In REFPROP 10.0, the Helmholtz energy equations of state (Kunz et al., 2007) are used to calculate the thermodynamic properties of mixtures containing refrigerants. For the description of the thermodynamic behaviour of a mixture, the Helmholtz energy model uses reducing functions depending on a set of binary interaction parameters ($\beta_{T,ij}$, $\gamma_{T,ij}$, $\beta_{v,ij}$, $\gamma_{v,ij}$), which need to be tuned with experimental data.

$$p = \rho RT\left(1 + \delta\frac{\partial\alpha^r}{\partial\delta}(\tau,\delta)\right) \quad (1)$$

$$\delta = \rho/\rho_{c(\bar{x})} \quad (2)$$

$$\tau = T_{c(\bar{x})}/T \quad (3)$$

$$T_{c,ij} = \beta_{T,ij}\gamma_{T,ij}\frac{x_i + x_j}{\beta_{T,ij}^2 x_i + x_j}\left(T_{c,i}T_{c,j}\right)^{1/2} \quad (4)$$

$$\frac{1}{\rho_{c,ij}} = \beta_{v,ij}\gamma_{v,ij}\frac{x_i + x_j}{\beta_{v,ij}^2 x_i + x_j}\frac{1}{8}\left(\frac{1}{\rho_{c,i}^{1/3}} + \frac{1}{\rho_{c,j}^{1/3}}\right)^3 \quad (5)$$

where *p*, ρ and *T* represent pressure, density and temperature of the mixture, respectively. Then, *x* is the molar fraction of the *i th* or *j-th* component of the mixture; α^r is the residual part of the dimensionless Helmholtz free energy. The model is built as a function of the reduced temperature τ and reduced density δ. Subscript *c* is referred to the critical conditions, while subscripts *T* and *v* are referred to temperature and volume for the binary interaction parameters.

In the case of a small amount of available data, binary interaction

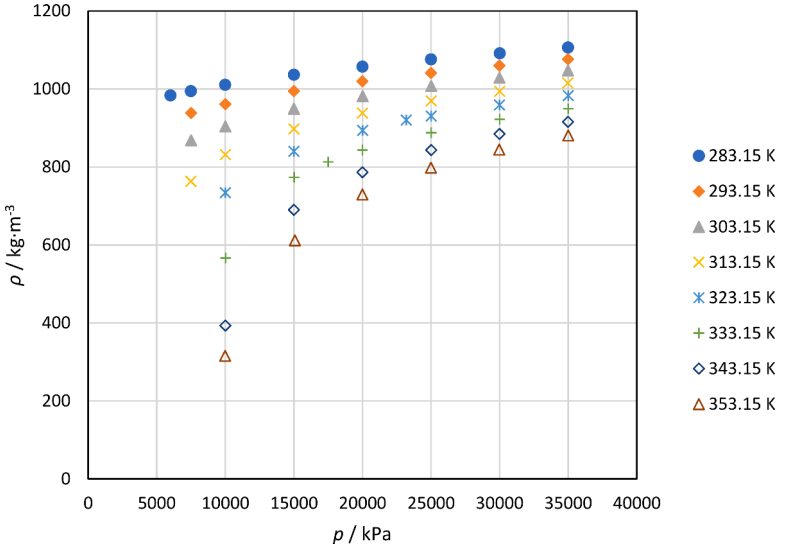

Fig. 3. Measured compressed liquid density (ρ) as function of pressure (p) for the ternary mixture.

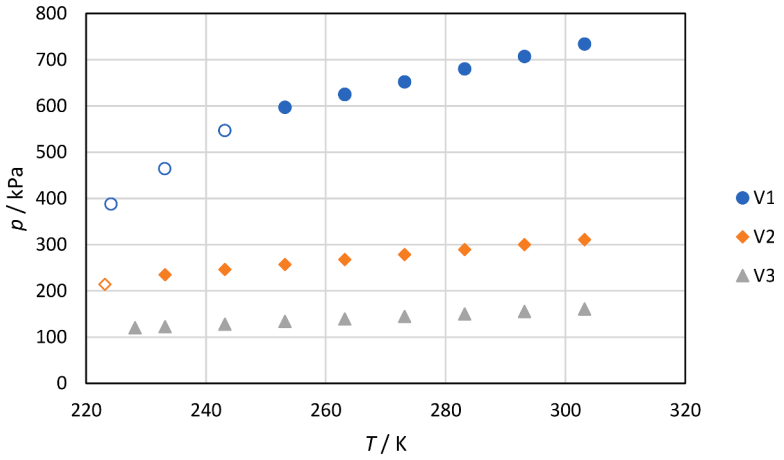

Fig. 4. Two-phase and superheated vapour pvTx properties for the ternary mixture where p is the pressure, v is the specific volume, T is the temperature, and x is the mixture composition. V1, V2 and V3 refer to the measured specific volumes which are equal to 0.060 $m^3 \bullet kg^{-1}$, 0.155 $m^3 \bullet kg^{-1}$ and 0.300 $m^3 \bullet kg^{-1}$, respectively. Empty points are in two-phase region.

Table 6
Two-phase values of pressure (p) temperature (T) and specific volume (v) for CO_2(1)/R32(2)/R134a(3) ternary mixture with overall experimental mass fractions of $w_1 = 0.684$, $w_2 = 0.117$, and $w_3 = 0.199$.[a].

T/K	*p*/kPa	*v*/$m^3 \bullet kg^{-1}$
224.15	387.7	0.0641
233.15	464.1	0.0642
243.15	546.5	0.0642
223.15	214.0	0.1553

[a] Standard uncertainties are $u(T) = 0.015$ K, $u(p) = 0.5$ kPa, $u(w_1) = u(w_2) = 0.005$, $u(v) = 0.0045$ $m^3 \bullet kg^{-1}$.

Table 7
Superheated vapour values of pressure(p) temperature (T) and specific volume (v) for CO_2 (1)/R32(2)/R134a(3) ternary mixture with overall experimental mass fractions of $w_1 = 0.684$, $w_2 = 0.117$, and $w_3 = 0.199$.[a].

T/K	*p*/kPa	*v*/$m^3 \bullet kg^{-1}$
253.15	597.4	0.0642
263.15	625.5	0.0643
273.15	652.4	0.0643
283.15	680.2	0.0643
293.15	707.4	0.0643
303.15	734.3	0.0644
233.15	234.9	0.1554
243.15	246.1	0.1555
253.15	256.9	0.1555
263.15	267.9	0.1556
273.15	278.5	0.1557
283.15	289.2	0.1557
293.15	300.1	0.1558
303.15	310.8	0.1559
228.15	120.0	0.2998
233.15	122.6	0.2998
243.15	128.2	0.3000
253.15	133.7	0.3001
263.15	139.2	0.3002
273.15	144.7	0.3004
283.15	150.0	0.3005
293.15	155.5	0.3006
303.15	160.9	0.3008

[a] Standard uncertainties are $u(T) = 0.015$ K, $u(p) = 0.5$ kPa, $u(w_1) = u(w_2) = 0.005$, $u(v) = 0.0165$ $m^3 \bullet kg^{-1}$.

parameters (BIPs) are set to 1. While, in the case of a significant amount of reliable data, an additional departure function can be used to obtain a more accurate fit of the data. To calculate the thermodynamic properties of a mixture with more than two components, as in this work, the superposition of the effects of all the pairs of pure fluids making up the mixture is applied.

The density calculation with REFPROP 10.0 using the default BIPs (reported in Table 10) was performed through the flash calculation subroutines with temperature, pressure, and composition as inputs. For compressed liquid density, the root mean square error (RMSE) was equal to 1.16%; while a RMSE equal to 1.22% was obtained for *pvTx* properties. Fig. 5 shows the deviations between the compressed liquid density measurements and the values provided by REFPROP 10.0; these deviations are calculated as:

$$\Delta\rho = \frac{(\rho_{calc} - \rho_{exp})}{\rho_{exp}} \tag{6}$$

where subscripts *exp* and *calc* are referred to experimentally measured density and calculated value, respectively.

Fig. 6 shows the deviations between the superheated vapour and two-phase densities and REFPROP 10.0 calculations. It is worth noticing that the values calculated by REFPROP 10.0 are always lower than the corresponding measured ones.

4.2. Binary interaction parameter tuning

While the BIPs already available in REFPROP 10.0 for R32/R134a binary system were considered accurate enough (Lemmon and Jacobsen, 2004), the default BIPs for CO_2/R32 and CO_2/R134a binary systems are predicted (they were not tuned on experimental data), since the amount of available data was limited (Bell and Lemmon, 2016). However, an accurate description of the behaviours of the binary mixtures constituting the ternary mixture is necessary to forecast the properties of the latter (Kunz et al., 2007). Hence, in this work, the binary interaction parameters for CO_2/R32 and CO_2/R134a binary mixtures are tuned on the presented measurements and the experimental literature data. To enlarge the set of available data utilised for the regressing binary interaction parameters, some previous works concerning the measurement of vapour-liquid equilibria (VLE), one-phase and two-phase density, and specific heat at a constant pressure of binary mixtures CO_2/R32 and CO_2/R134a were considered. The selected works are shown in Tables 8 and 9.

The tuning of the parameters was performed through a heuristic algorithm, Adaptive Search Development Particle Swarm Optimization (ASD-PSO) (Ardizzon et al., 2015), whose aim was to minimise the objective function, *f*, consisting of a weighted mean value of root mean square (RMS) calculated for molar fraction (x and y), density (ρ) and

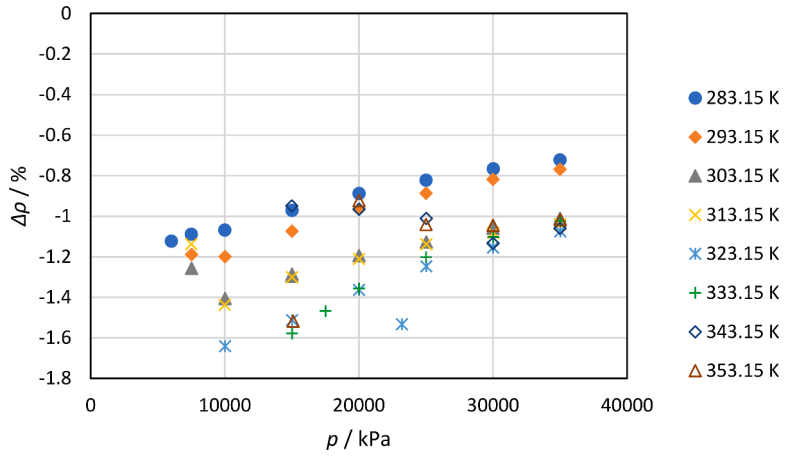

Fig. 5. Deviations between compressed liquid density experimental measurements and REFPROP 10.0 calculations (Δρ) as function of pressure (p).

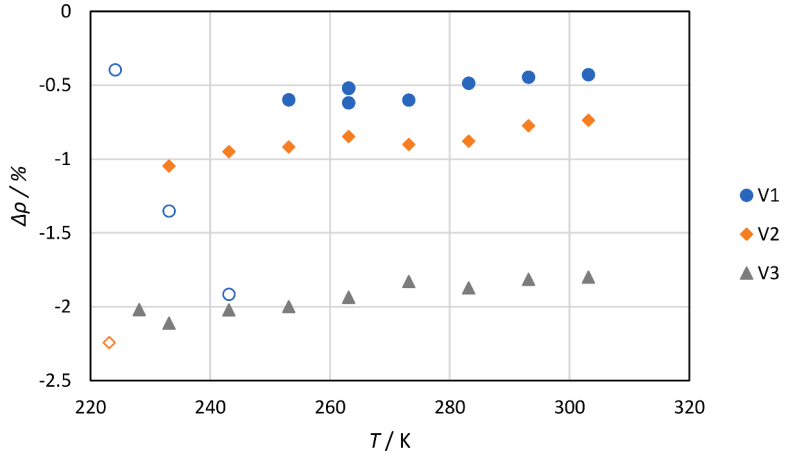

Fig. 6. Deviations between vapour-phase and two-phase measured densities and REFPROP 10.0 calculations (Δρ) as a function of temperature (T). V1, V2 and V3 refer to the specific volumes of the measured isochores which are equal to 0.060 $m^3 \bullet kg^{-1}$, 0.155 $m^3 \bullet kg^{-1}$ and 0.300 $m^3 \bullet kg^{-1}$, respectively. Empty points refer to two-phase region.

Table 8
Experimental data for CO_2/R32 binary system available in the literature.

Reference	Type	Amount of experimental data
Diefenbacher and Türk (2002)	VLE	9
Rivollet et al. (2004)	VLE	45
Stein and Adams (1971)	VLE	48
Di Nicola et al. (2002)	VLE	5
Arami-Niya et al. (2020)	VLE	5
Di Nicola et al. (2002)	Density	65
Arami-Niya et al. (2020)	Density	9
Arami-Niya et al. (2020)	Specific Heat	9

Table 9
Experimental data for CO_2/R134a binary system available in the literature.

References	Type	Amount of experimental data
Duran-Valencia et al. (2002)	VLE	27
Lim et al. (2008)	VLE	37
Silva-Oliver and Galicia-Luna (2002)	VLE	23
Arami-Niya et al. (2020)	VLE	5
Arami-Niya et al. (2020)	Density	7
Arami-Niya et al. (2020)	Specific Heat	8

specific heat at constant pressure (c_p):

$$f = W_{VLE}\,RMS(VLE) + W_{\rho}RMS(\rho) + W_{cp}RMS(c_p) \tag{7}$$

where:

$$RMS(VLE) = \sqrt{\frac{1}{N}\sum_i \left(x_{exp,i} - x_{calc,i}\right)^2 + \left(y_{exp,i} - y_{calc,i}\right)^2} \tag{8}$$

$$RMS(\rho) = \sqrt{\frac{1}{N}\sum_i \left(\frac{\rho_{exp,i} - \rho_{calc,i}}{\rho_{exp,i}}\right)^2} \tag{9}$$

$$RMS(cp) = \sqrt{\frac{1}{N}\sum_i \left(\frac{cp_{exp,i} - cp_{calc,i}}{cp_{exp,i}}\right)^2} \tag{10}$$

Thermodynamic properties are computed by REFPROP 10.0 subroutines. W_{VLE}, W_{ρ} and W_{cp} are the weighting factors related to the properties which are chosen empirically on the basis of RMS deviations magnitude, the accuracy of experimental data and the sensitivity of BIPs to each property. Following these considerations, W_{VLE}, W_{ρ} and W_{cp} are set to 1, 5, and 0.1, respectively.

Binary interaction parameters obtained by the tuning are shown in Table 10.

Table 11 shows a comparison between the accuracy of the models with REFPROP 10.0 default BIPs and tuned parameters with respect to

Table 10
Comparison between binary REFPROP 10.0 default values and tuned binary interaction parameters ($\beta_{T,ij}$, $\gamma_{T,ij}$, $\beta_{v,ij}$, $\gamma_{v,ij}$).

	REFPROP 10.0 default values				Tuned values			
	$\beta_{T,ij}$	$\gamma_{T,ij}$	$\beta_{v,ij}$	$\gamma_{v,ij}$	$\beta_{T,ij}$	$\gamma_{T,ij}$	$\beta_{v,ij}$	$\gamma_{v,ij}$
CO_2/R32	1	0.99782	1	1.0059	0.99246	0.99597	1.1	0.98595
CO_2/R134a	1	1.008	1	1	0.98585	1.00445	0.99217	1.0294
R134a/R32	1	1.0144	1	1.0137	–	–	–	–

Table 11
Accuracy comparison between default and tuned BIPs.

CO_2/R32/R134a				
			RMSE	
Reference	Property	Amount of experimental data	REFPROP 10.0	Tuned parameters
This work	*pvTx*	37	1.22%	1.30%
This work	Density	53	1.16%	0.213%
CO_2/R32				
			RMSE	
Reference	Property	Amount of experimental data	REFPROP 10.0	Tuned parameters
Diefenbacher and Türk (2002)	VLE	9	0.0146	0.0144
Rivollet et al. (2004)	VLE	45	0.0097	0.0080
Stein and Adams (1971)	VLE	48	0.0125	0.0122
Di Nicola et al. (2002)	VLE	5	0.0130	0.0100
Arami-Niya et al. (2020)	VLE	5	0.0115	0.0090
Di Nicola et al. (2002) *	Density	65	1.22%	0.63%
Arami-Niya et al. (2020)	Density	9	1.15%	0.18%
Arami-Niya et al. (2020)	Specific Heat	9	3.11%	2.98%
CO_2/R134a				
			RMSE	
Reference	Property	Amount of experimental data	REFPROP 10.0	Tuned parameters
Duran-Valencia et al. (2002)	VLE	27	0.0112	0.0331
Lim et al. (2008)	VLE	37	0.0698	0.0539
Silva-Oliver and Galicia-Luna (2002)	VLE	23	0.0497	0.0275
Arami-Niya et al. (2020)	VLE	5	0.0156	0.0380
Arami-Niya et al. (2020)	Density	7	1.59%	2.16%
Arami-Niya et al. (2020)	Specific Heat	8	3.77%	3.72%

* for this refence, only the data in the superheated vapour conditions have been considered in the fitting.

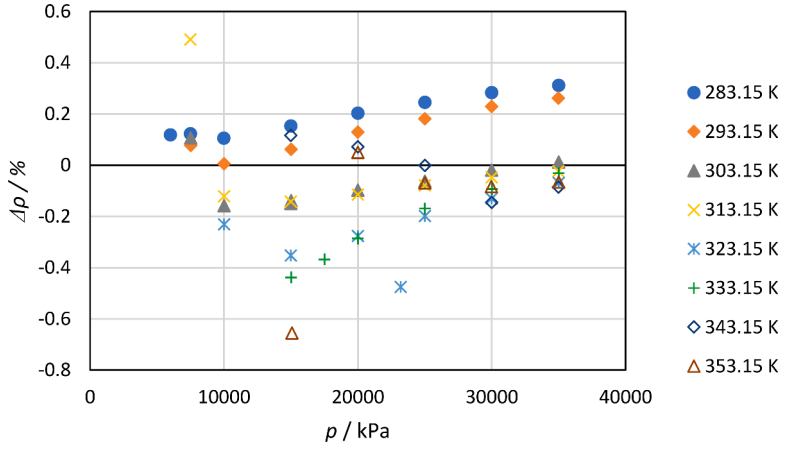

Fig. 7. Deviations between compressed liquid density experimental measurements and calculations with tuned binary interaction parameters (Δρ) as a function of pressure (p).

the measurements on the ternary mixture performed in this work and all the datasets used to tune the new BIPs. As it can be noticed, a significant improvement in accuracy was obtained for the compressed liquid density of the ternary mixture, while only a slight increase was obtained in error on *pvTx* measurements. This can be due to the lower number of *pvTx* data considered in the tuning of the parameters. Another reason could involve the presence of a few points in two-phase region where the model seemed less accurate in the density calculation. As far as the other datasets are concerned, a general improvement is obtained for the blend of CO_2/R32. For some of the CO_2/R134a datasets, the new parameters caused a slight increase in the deviations. However, from a global point of view, the new parameters tuned within this work can be considered more accurate than the REFPROP 10.0 default BIPs. Figs. 7 and 8 show the deviations between experimental measurements and properties calculated with tuned binary interaction parameters for both experiments. Also, from these figures, it is evident that the tuned BIPs especially ensured lower deviations between the measurements of compressed liquid density and calculated values than those provided by the default BIPs.

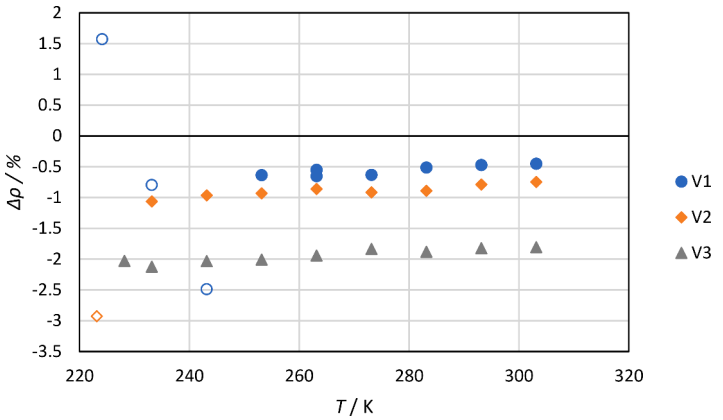

Fig. 8. Deviations between vapour-phase and two-phase measured density and calculations with tuned binary interaction parameters (Δρ) as a function of temperature (T). V1, V2 and V3 refer to the specific volumes of the measured isochores which are equal to 0.060 m3•kg−1, 0.155 m3•kg−1 and 0.300 m3•kg−1, respectively. Empty points refer to two-phase region.

Table 12
Technical specifics of DM1200C (ACS, 2022).

Parameters	Values
Useful capacity (l)	1076
Temperature Range (K)	From 198 to 453
Temperature Fluctuation (K)	From ±0.1 to ±0.3
Temperature changing rate Heating[a]	4.5 K/min
Temperature changing rate Cooling[a]	2.3 K/min
Humidity range (%)	From 10 to 98
Temperature range for climatic test (K)	From 283 to 368
Humidity Fluctuation (%)	From ±1 to ±3
Maximum thermal Load (W)	3000

[a] According to IEC 60,068–3–5 and IEC 60,068–3–6, at ambient temperature without specimen.

5. Experimental testing of R472A

The mixture was tested in a DM1200C ACS chamber (ACS, 2022). It is an environmental simulation chamber which allows to perform temperature test cycles from 453 K down to 198 K according to several test specifications requiring a high grade of repeatability (temperature fluctuation lower than ± 1 K). The chamber specifics are reported in Table 12. amongst the listed parameters, the temperature-changing rate for cooling of the chamber is a fundamental feature for this kind of devices. This characteristic is strictly dependant on the heat exchange capacity of the adopted refrigerant.

The performance of R472A was evaluated by running a test of the temperature changing rate during cooling. The test was carried out by assessing the gradient from 453.15 K to 198.15 K (i.e., the maximum and minimum temperature of this model, respectively). In particular, the chamber temperature was set at 453.15 K for 2 h (stabilisation time), then lowered to 203.15 K at maximum speed. The stabilisation time helps to guarantee the temperature homogeneity within the useful volume of the chamber. Properties such as temperature, humidity, low-stage pressure, and high-stage pressure were recorded and analysed using the chamber's internal software, MyKratos. Then, these data were compared to that recorded during the test performed on the chamber with the bottoming cycle of the refrigeration system filled with R23.

As illustrated in Fig. 9, the first section of the blue curve (R472A) has a greater gradient than the orange curve (R23), showing a better cooling rate change. Therefore, this means an improvement of heat exchange capacity of R472A. However, it can be noted that at low temperatures (around 213.15 K), R23 shows better performances. Overall, the comparison reveals a temperature changing rate during cooling of 3.6 K/min (according to IEC60068–3–5/6) for R472A, with a 20% improvement with respect to R23.

6. Conclusions

This paper presents *pvTx* measurements for the ternary system consisting of 69 mass% of CO_2, 12 mass% of R32, and 19 mass% of R134a carried out in the compressed liquid, superheated vapour, and two-

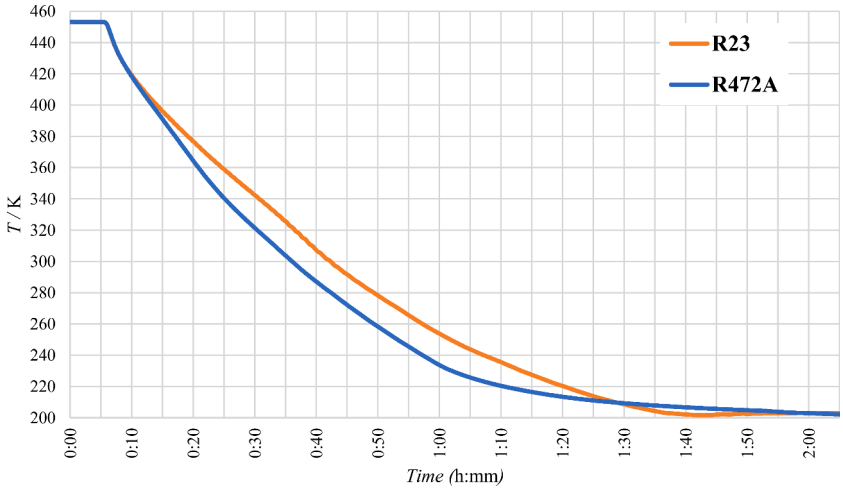

Fig. 9. Cooling change rate comparison between R23 and R472A in DM chamber.

phase regions. A vibrating tube densimeter was used to measure the compressed liquid density along 8 isotherms from (283.15 to 353.15) K and for pressures from close to saturation up to 35 MPa. An isochoric apparatus was used to carry out *pvTx* measurements in the two-phase and superheated vapour regions along 3 isochores from (223.15 to 303.15) K. The presented experimental data were compared with the calculations provided by the multi-fluid Helmholtz-energy explicit model using the default binary interaction parameters available in REFPROP 10.0. The model provided a RMSE of 1.16% for the compressed liquid density measurements and a RMSE of 1.22% for the two-phase and the superheated vapour *pvTx* data. In addition, this model was tested using new binary interaction parameters tuned to the presented data and the literature experimental thermodynamic properties of the binary mixtures constituting the ternary mixture. The tuned parameters provided better results than those of the default parameters used in REFPROP 10.0 for the compressed liquid density data (RMSE = 0.213%) and a slight increase for the *pvTx* data (RMSE =1.30%). From the results of experimental tests using an environmental simulation chamber, it was found that R472A had a changing rate cooling of 3.6 K/min, which was a 20% improvement with respect to R23.

Funding

This research did not receive any specific grant from funding agencies in the public, commercial, or not-for-profit sectors.

Declaration of Competing Interest

The authors declare that they have no known competing financial interests or personal relationships that could have appeared to influence the work reported in this paper.

Acknowledgements

The authors of the paper would like to thank Mauro Scattolini, National Research Council (CNR), Construction Technologies Institute (ITC), Padova, Italy, for the effective cooperation to the experimental measurement.

References

ACS, 2022, Climatic chamber model DM1200 C. URL: https://acs.angelantoni.com/en/news/dm1200c-discoverymy-climatic-chamber (accessed 7 October 2022).

Arami-Niya, A., Xiao, X., Al Ghafri, S.Z.S., Jiao, F., Khamphasith, M., Pouya, E.S., Sadaghiani, M.S., Yang, X., Tsuji, T., Tanaka, Y., Seiki, Y., May, E.F., 2020. Measurement and modelling of the thermodynamic properties of carbon dioxide mixtures with HFO-1234yf, HFC-125, HFC-134a, and HFC-32: vapour-liquid equilibrium, density, and heat capacity. Int. J. Refrig. 118, 514–528.

Ardizzon, G., Cavazzini, G., Pavesi, G., 2015. Adaptive acceleration coefficients for a new search diversification strategy in particle swarm optimisation algorithms. Inf. Sci. (Ny). 299, 337–378.

ASHRAE, A., 2019. Standard 34-2019, Designation and safety classification of refrigerants. Am. Soc. heating, Refrig. Air-Conditioning Eng. Atlanta, GA.

Bell, I.H., Lemmon, E.W., 2016. Automatic fitting of binary interaction parameters for multi-fluid Helmholtz-energy-explicit mixture models. J. Chem. Eng. Data 61, 3752–3760.

Bobbo, S., Fedele, L., Scattolini, M., Camporese, R., 2002. Compressed liquid densities, saturated liquid densities, and vapor pressures of hexafluoro-1, 3-butadiene (C4F6). J. Chem. & Eng. Data 47, 179–182.

Bobbo, S., Scattolini, M., Fedele, L., Camporese, R., 2004. Compressed liquid densities and saturated liquid densities of HFC-365mfc. Fluid Phase Equilib 222, 291–296.

Brown, J.S., Coccia, G., Tomassetti, S., Pierantozzi, M., Di Nicola, G., 2018. Vapor phase *PvTx* measurements of binary blends of trans-1-Chloro-3,3,3-trifluoroprop-1-ene + Isobutane and cis-1,3,3,3-Tetrafluoroprop-1-ene + Isobutane. J. Chem. Eng. Data 63, 169–177. https://doi.org/10.1021/acs.jced.7b00769.

Brown, J.S., Coccia, G., Tomassetti, S., Pierantozzi, M., Di Nicola, G., 2017. Vapor phase *PvTx* measurements of binary blends of 2,3,3,3-Tetrafluoroprop-1-ene + Isobutane and trans-1,3,3,3-Tetrafluoroprop-1-ene + Isobutane. J. Chem. Eng. Data 62, 3577–3584. https://doi.org/10.1021/acs.jced.7b00564.

Di Nicola, G., Giuliani, G., Polonara, F., Stryjek, R., 2005a. Blends of carbon dioxide and HFCs as working fluids for the low-temperature circuit in cascade refrigerating systems. Int. J. Refrig. 28, 130–140.

Di Nicola, G., Pacetti, M., Polonara, F., Stryjek, R., 2002. Isochoric measurements for CO2+ R125 and CO2+ R32 binary systems. J. Chem. & Eng. Data 47, 1145–1153.

Di Nicola, G., Polonara, F., Ricci, R., Stryjek, R., 2005b. *PVTx* measurements for the R116 + CO_2 and R41+ CO_2 systems. New isochoric apparatus. J. Chem. Eng. Data 50, 312–318.

Di Nicola, G., Polonara, F., Stryjek, R., Arteconi, A., 2011. Performance of cascade cycles working with blends of CO_2+ natural refrigerants. Int. J. Refrig. 34, 1436–1445.

Diefenbacher, A., Türk, M., 2002. Vapour+ liquid) Equilibria of binary mixtures of CO2, CH2F2, CHF3, and SF6. J. Chem. Thermodyn. 34, 1361–1375.

Duran-Valencia, C., Pointurier, G., Valtz, A., Guilbot, P., Richon, D., 2002. Vapor- liquid equilibrium (VLE) data for the carbon dioxide (CO_2)+ 1, 1, 1, 2-tetrafluoroethane (R134a) system at temperatures from 252.95K to 292.95K and pressures up to 2MPa. J. Chem. & Eng. Data 47, 59–61.

Fedele, L., Pierantozzi, M., Di Nicola, G., Brown, J.S., Bobbo, S., 2018. Compressed liquid density and vapor phase *pvt* measurements of trans-1-chloro-3, 3, 3-trifluoroprop-1-ene [r1233zd (e)]. J. Chem. & Eng. Data 63, 225–232.

Giuliani, G., Kumar, S., Polonara, F., 1995. A constant volume apparatus for vapour pressure and gas phase P-ν-T measurements: validation with data for R22 and R134a. Fluid Phase Equilib 109, 265–279. https://doi.org/10.1016/0378-3812(95)02727-V.

Kim, D., Yang, X., Arami-Niya, A., Rowland, D., Xiao, X., Al Ghafri, S.Z.S., Tsuji, T., Tanaka, Y., Seiki, Y., May, E.F., 2020. Thermal conductivity measurements of refrigerant mixtures containing hydrofluorocarbons (HFC-32, HFC-125, HFC-134a), hydrofluoroolefins (HFO-1234yf), and carbon dioxide (CO2). J. Chem. Thermodyn. 151, 106248.

Kunz, O., Klimeck, R., Wagner, W., Jaeschke, M., 2007. The GERG-2004 wide-range equation of state for natural gases and other mixtures.

Lemmon, E.W., Jacobsen, R.T., 2004. Equations of state for mixtures of R-32, R-125, R-134a, R-143a, and R-152a. J. Phys. Chem. Ref. data 33, 593–620.

Lim, J.S., Jin, J.M., Yoo, K.P., 2008. VLE measurement for binary systems of CO_2+ 1, 1, 1, 2-tetrafluoroethane (HFC-134a) at high pressures. J. Supercrit. Fluids 44, 279–283.

Mota-Babiloni, A., Joybari, M.M., Navarro-Esbrì, J., Mateu-Royo, C., Barragán-Cervera, Á., Amat-Albuixech, M., Molés, F., 2020. Ultralow-temperature refrigeration systems: configurations and refrigerants to reduce the environmental impact. Int. J. Refrig. 111, 147–158.

Regulation (EU) No. 517/2014, 2014. Regulation (EU) No 517/2014 of the European parliament and of the council of 16 April 2014 on fluorinated greenhouse gases and repealing regulation (EC) No 842/2006. Official Journal of the European Union.

Rivollet, F., Chapoy, A., Coquelet, C., Richon, D., 2004. Vapor–liquid equilibrium data for the carbon dioxide (CO_2)+ difluoromethane (R32) system at temperatures from 283.12 to 343.25K and pressures up to 7.46MPa. Fluid Phase Equilib. 218, 95–101.

Santos, A.F., Gaspar, P.D., de Souza, H.J.L., 2021. Refrigeration of COVID-19 vaccines: ideal storage characteristics, energy efficiency and environmental impacts of various vaccine options. Energies 14, 1849.

Silva-Oliver, G., Galicia-Luna, L.A., 2002. Vapor–liquid equilibria for carbon dioxide + 1, 1, 1, 2-tetrafluoroethane (R-134a) systems at temperatures from 329 to 354K and pressures upto 7.37MPa. Fluid Phase Equilib. 199, 213–222.

Stein, F.P., Adams, R.A., 1971. Vapor-liquid equilibriums for carbon dioxide-difluoromethane system. J. Chem. & Eng. Data 16, 146–149.

Sun, J., Zhang, M., Gehl, A., Fricke, B., Nawaz, K., Gluesenkamp, K., Shen, B., Munk, J., Hagerman, J., Lapsa, M., 2021. COVID 19 vaccine distribution solution to the last mile challenge: experimental and simulation studies of ultra-low temperature refrigeration system. Int. J. Refrig.

UNEP, 2016. Amendment to the montreal protocol on substances that deplete the ozone layer (Kigali Amendment). Int. Leg. Mater. https://doi.org/10.1017/ilm.2016.2.

Wagner, W., Pruß, A., 2002. The IAPWS formulation 1995 for the thermodynamic properties of ordinary water substance for general and scientific use. J. Phys. Chem. Ref. Data 31, 387–535.

Yang, X., Arami-Niya, A., Xiao, X., Kim, D., Al Ghafri, S.Z.S., Tsuji, T., Tanaka, Y., Seiki, Y., May, E.F., 2020. Viscosity measurements of binary and multicomponent refrigerant mixtures containing HFC-32, HFC-125, HFC-134a, HFO-1234yf, and CO2. J. Chem. & Eng. Data 65, 4252–4262.